



# A facile preparation of Ag<sub>2</sub>O/P25 photocatalyst for selective reduction of nitrate



Hai-Tao Ren<sup>a</sup>, Shao-Yi Jia<sup>a</sup>, Ji-Jun Zou<sup>a</sup>, Song-Hai Wu<sup>a</sup>, Xu Han<sup>b,c,\*</sup>

<sup>a</sup> School of Chemical Engineering and Technology, Tianjin University, Tianjin, PR China

<sup>b</sup> School of Environmental Science and Engineering, Tianjin University, Tianjin, PR China

<sup>c</sup> Key Laboratory of Systems Bioengineering, Ministry of Education, Tianjin University, Tianjin, PR China

## ARTICLE INFO

### Article history:

Received 30 January 2015

Received in revised form 17 March 2015

Accepted 23 March 2015

Available online 24 March 2015

### Keywords:

Ag(0)

Ag<sub>2</sub>O

Titanium dioxide

Photocatalysis

Selective nitrate reduction

## ABSTRACT

Ag<sub>2</sub>O/P25 and Ag/P25 catalysts were synthesized and applied in the photocatalytic reduction of nitrate with formic acid as a hole scavenger. X-ray diffraction (XRD), X-ray photoelectron spectroscopy (XPS) and transmission electron microscope (TEM) analysis demonstrate that Ag<sub>2</sub>O or Ag nanoparticles were well distributed on the surface of P25. Under UV irradiation, 5% Ag<sub>2</sub>O/P25 showed a fast rate (0.95 h<sup>-1</sup>, 6.3 times of P25), a high conversion (97.2%, 3.63 times of P25) and a high N<sub>2</sub> selectivity (83.1%, 1.15 times of P25) for nitrate reduction. The improved separation of electron–hole pairs on Ag<sub>2</sub>O/P25 results in the high conversion of nitrate. Moreover, compared with the Ag/P25 catalyst, Ag<sub>2</sub>O/P25 exhibited a good reusability in nitrate reduction. The formed Ag–Ag<sub>2</sub>O structure [Ag(0) present on the surface of Ag<sub>2</sub>O] over P25 by partial photoreduction of deposited Ag<sub>2</sub>O contributed to the better stability of Ag<sub>2</sub>O/P25 in nitrate reduction. The present study provides a new sight into the use of Ag<sub>2</sub>O/P25 catalyst in the reduction of nitrate.

© 2015 Elsevier B.V. All rights reserved.

## 1. Introduction

With the utilization of soluble nitrogen-based fertilizers, consumption of animal products and production of nitrogen contained wastewater, more nitrate (NO<sub>3</sub><sup>-</sup>) is being discharged into rivers and lakes [1]. In addition of eutrophication caused by nitrate pollution, nitrate and its metabolites, particularly nitrite (NO<sub>2</sub><sup>-</sup>) produced from the reduction of nitrate, are toxic to human beings. Previous studies suggested that nitrate could combine with hemoglobin to form methemoglobin and caused blue baby syndrome, and nitrosamine formed from nitrite could also cause hypertension and cancers [1,2]. Considering the toxicity of nitrate and its metabolites to human beings, the U.S. Environmental Protection Agency (EPA) has set the maximum allowable contamination level of 10 mg L<sup>-1</sup> of nitrate–nitrogen (NO<sub>3</sub>-N) in drinking water [3].

Removal of nitrate from wastewater presents a challenge due to its high stability and solubility. Although nitrate can be efficiently eliminated from water by ion exchange, reverse osmosis and electrodialysis, further treatment of the produced brines are required [4–6]. In contrast, biological treatments allow the reduction of

nitrate into harmless nitrogen gas (N<sub>2</sub>). However, these processes are inherently slow, difficult to handle, and cannot meet the high removal requirement of nitrate [7]. A chemical catalytic process can efficiently reduce nitrate to N<sub>2</sub>. The pioneer work of Vorlop and Tacke [8] demonstrated that catalytic reduction by hydrogen gas could efficiently reduce nitrate to N<sub>2</sub> over Pd–Cu bi-metallic catalyst. After that, numerous studies aimed to develop new catalysts, supports, reducing agents and reactor configurations in the reduction of nitrate [9,10]. Nevertheless, activity and selectivity for nitrate transformation cannot be simultaneously satisfied.

In recent years, heterogeneous photocatalytic reduction of nitrate over semiconductor materials attracts more attention. Among them, titania (TiO<sub>2</sub>) and metal-loaded (such as Pt [11–13], Pd [12–14], Rh [13], Ru [13], Au [15,16] and Ag [17–19]) TiO<sub>2</sub> are widely used and effective in the reduction of nitrate with a high selectivity toward N<sub>2</sub> [12,17–19]. Metallic Ag(0) is a good co-catalyst for nitrate reduction because it can act as electron trap due to the formed Schottky barrier, drawing electrons and leaving the holes on the bulk TiO<sub>2</sub> as well as enhancing the separation time of electrons and holes [17–20]. Zhang et al. [17] prepared Ag/TiO<sub>2</sub> catalyst with a selectivity of 100% toward N<sub>2</sub>, which showed one order of magnitude higher activity than the hydrogenation catalysts. However, our preliminary results found that catalytic ability of this catalyst decreased significantly in the second cycle, and this requires the development of new catalysts with a good

\* Corresponding author at: School of Environmental Science and Engineering, Tianjin University, Tianjin, PR China. Tel.: +86 15222072695.

E-mail address: [xuhan@tju.edu.cn](mailto:xuhan@tju.edu.cn) (X. Han).

reusability in the reduction of nitrate. Silver(I) oxide ( $\text{Ag}_2\text{O}$ ) is a p-type semiconductor with an energy band gap of 1.46 eV [21], and it has exhibited a good photocatalytic activity in the decomposition of organic contaminant [22,23]. We therefore, hypothesize that  $\text{Ag}_2\text{O}/\text{TiO}_2$  can also be used as an effective catalyst in the reduction of nitrate, and mechanism of photocatalytic reduction of nitrate should be different from that of  $\text{Ag}/\text{TiO}_2$ .

In nitrate reduction, the addition of organic compounds (such as alcohols [13] and carboxylic acids [12,17–19,24,25]) is always required to fill valence band holes (i.e., electron donor or hole scavenger), to decrease recombination of electrons and holes on  $\text{TiO}_2$ , or to produce radicals to reduce nitrate. It has been proved that formic acid ( $\text{HCOOH}$ ) is the most efficient hole scavenger for nitrate reduction on  $\text{Ag}/\text{TiO}_2$  [17,19]. Mechanisms involved in photocatalytic reduction of nitrate by  $\text{Ag}/\text{TiO}_2$  are always thought to occur via reaction with  $\text{CO}_2^{\bullet-}$  radical produced from the reaction between photo-generated holes and formic acid [17,19,26], or by direct interaction of nitrate with electrons on the surface of photocatalysts [18].

In this study,  $\text{Ag}_2\text{O}/\text{TiO}_2$  and  $\text{Ag}/\text{TiO}_2$  catalysts are successfully prepared through a pH-mediated chemical precipitation reaction and a pH-mediated chemical reduction method, respectively. The objectives of this study are to investigate: (i) the photocatalytic activity and selectivity of nitrate reduction by  $\text{Ag}_2\text{O}/\text{TiO}_2$ , (ii) the reusability of  $\text{Ag}_2\text{O}/\text{TiO}_2$  and  $\text{Ag}/\text{TiO}_2$  in the photocatalytic reduction of nitrate, and (iii) different mechanisms involved in the photocatalytic reduction of nitrate over  $\text{Ag}_2\text{O}/\text{TiO}_2$  and  $\text{Ag}/\text{TiO}_2$ .

## 2. Experimental

### 2.1. Chemicals

In this study,  $\text{TiO}_2$  was commercially available Degussa P25 (Germany) with a surface area of ca.  $50 \text{ m}^2 \text{ g}^{-1}$ , including two phases of anatase (80%) and rutile (20%). Other chemicals of analytical grade were used without further purification.

### 2.2. Catalyst preparation

$\text{Ag}/\text{P25}$  and  $\text{Ag}_2\text{O}/\text{P25}$  catalysts were prepared through a pH-mediated chemical reduction method and a pH-mediated chemical precipitation reaction, respectively. Typically, 0.3 g P25 was dispersed in 35 mL deionized water and stirred for 4 h, and then 0.03 mL of 0.5 M NaOH was added to adjust the pH of the suspension to 8.45. Subsequently, a measured amount of 0.2 M  $\text{AgNO}_3$  was dropwise into the suspension. The mixture was stirred in dark for 30 min to reach  $\text{Ag}^+$  sorption equilibrium.

In the preparation of  $\text{Ag}_2\text{O}/\text{P25}$ , a measured amount of 0.5 M NaOH solution was slowly added into the  $\text{Ag}^+$  pre-equilibrated mixture. The mixture was stirred at room temperature for 1 h, and then centrifuged and washed repeatedly with deionized water for three times and ethanol for twice. The obtained pellets were then freeze-dried and labeled as  $x\% \text{ Ag}_2\text{O}/\text{P25}$ , where  $x$  is the weight ratio of  $\text{Ag}_2\text{O}$  to P25. Different catalysts of 1–20%  $\text{Ag}_2\text{O}/\text{P25}$  were prepared by varying the amount of  $\text{AgNO}_3$  and NaOH.

In the preparation of  $\text{Ag}/\text{P25}$ , 1.40 mL of 0.1 M  $\text{NaBH}_4$  (prepared in 0.1 M NaOH aqueous solution) was slowly added into the  $\text{Ag}^+$  – preloaded mixture after purging with high purity  $\text{N}_2$  for 15 min. Other procedures were the same as the preparation of  $\text{Ag}_2\text{O}/\text{P25}$ . The obtained pellets were then freeze-dried and denoted as F- $\text{Ag}/\text{P25}$  (Fresh  $\text{Ag}/\text{P25}$ ). The Ag weight content of  $\text{Ag}/\text{P25}$  was 1%, as analyzed by ICP-AES (Varian-715, Varian, USA) at  $\lambda = 328.07 \text{ nm}$ . It has been demonstrated that 1%  $\text{Ag}/\text{TiO}_2$  catalyst showed the optimal activity and selectivity toward nitrate reduction [17]. In

addition, the synthetic F- $\text{Ag}/\text{P25}$  preserved for 1 month at room temperature was denoted as M- $\text{Ag}/\text{P25}$ .

### 2.3. Catalyst characterization

The crystalline structure of the synthetic  $\text{Ag}/\text{P25}$  and  $\text{Ag}_2\text{O}/\text{P25}$  was analyzed by X-ray diffraction (XRD, Rigaku D/max 2200/PC).  $\text{Ag}/\text{P25}$  and  $\text{Ag}_2\text{O}/\text{P25}$  were also characterized with high-resolution transmission electron microscopy (HRTEM, Fei Tecnai G2 F20) on a 2100 JEOL microscope (200 kV) using copper grids for the distribution and morphology of Ag and  $\text{Ag}_2\text{O}$  particles around P25. Oxidation states of Ag on P25 were determined by X-ray photoelectron spectra (XPS, Pe PHI-1600 ESCA) with a monochromatic Al K $\alpha$  radiation (1486.6 eV) and base pressure of  $1 \times 10^{-8}$  Torr in the analytical chamber. C1s peaks were used as an inner standard calibration peak at 284.8 eV. Photoluminescence (PL) spectra of the catalysts were recorded using a Fluorolog 3-21 photoluminescence spectrometer (Horiba Jobin Yvon, France) at room temperature. The excitation wavelength was 325 nm, and the range of 350–550 nm was recorded.

### 2.4. Photocatalytic testing

Photocatalytic experiments were carried out using a Model XPA-VII photocatalytic reactor (Xujiang Electromechanical Plant, Nanjing, China). A 300 W high pressure Hg lamp (main wavelength around 365 nm) placed in a quartz socket tube with one end closed was used as the light source. The distance between the light source and the reactor was 12 cm. The light intensity of Hg lamp was measured by a UV Radiometer (Photoelectric Instrument Factory of Beijing Normal University) at 365 nm and it was  $2.50 \text{ mW cm}^{-2}$  at the quartz tube spot. The temperature inside the reactor was maintained at  $21 \pm 1^\circ \text{C}$  by continuous circulation of cool water. A mixture of 20 mg catalyst ( $\text{Ag}_2\text{O}/\text{P25}$  or  $\text{Ag}/\text{P25}$ ) and 20 mL of nitrate ( $100 \text{ mg N L}^{-1}$ ) was stirred for 30 min in quartz tube (inner diameter = 2 cm, volume = 50 mL) in dark to reach sorption equilibrium of nitrate on the catalyst. Results demonstrated that the adsorption percentage of nitrate on  $\text{Ag}_2\text{O}/\text{P25}$  or  $\text{Ag}/\text{P25}$  was no more than 1%. No treatment was carried out to drive out the dissolved oxygen. Formic acid (0.8 mL, 0.2 M) was added to the suspension before irradiation. During irradiation, a measured amount of suspension was withdrawn regularly and centrifuged, and the supernatant was analyzed to determine the residual concentrations of nitrate, nitrite, and ammonium with colorimetric methods [27] by an UV-vis spectrophotometer (Mapada, UV-6300). Generally, nitrate was measured at 220 and 275 nm, nitrite at 540 nm, and ammonium at 420 nm. Control experiments without illumination demonstrated that nitrate reduction in dark was insignificant.

The catalytic activity for the reduction of nitrate is commonly defined as the amount of nitrate anion reduced in unit time and catalyst weight ( $\text{mg}_{\text{NO}_3^-} \text{ h}^{-1} \text{ g}_{\text{cat}}^{-1}$ ). Previous studies suggested that the major products in solution in the photocatalytic reduction of nitrate were nitrite, ammonium and  $\text{N}_2$  [14,17,19], and  $\text{N}_2$  selectivity was therefore calculated from the balance of nitrogen products analyzed in solution. The selectivity toward  $\text{N}_2$  (a) is defined as follows:

$$S(\text{N}_2-\text{N}) = \frac{[\text{NO}_3^-]_0 - [\text{NO}_3^-]_t - [\text{NO}_2^-]_t - [\text{NH}_4^+]_t}{[\text{NO}_3^-]_0 - [\text{NO}_3^-]_t} \quad (\text{a}),$$

where  $[\text{X}]_0$  and  $[\text{X}]_t$  are concentrations of nitrogen species at time 0 and  $t$ , respectively.

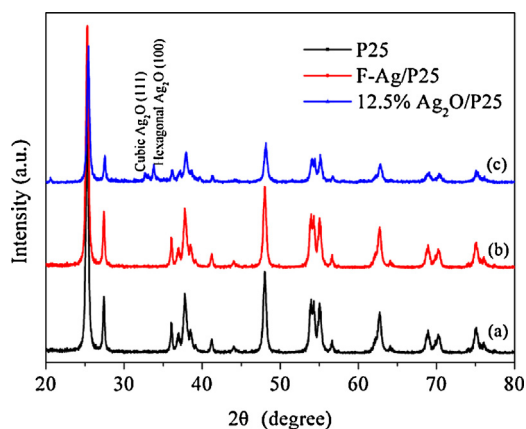


Fig. 1. XRD patterns of (a) P25, (b) F-Ag/P25 and (c) 12.5% Ag<sub>2</sub>O/P25.

### 3. Results and discussion

#### 3.1. Characterization of photocatalysts

XRD patterns illustrate the crystalline development of Ag<sub>2</sub>O/P25 and Ag/P25 synthesized in this study compared to neat P25. Neat P25 is composed of anatase (JCPDS No. 21-1272) and rutile (JCPDS No. 21-1276) phases (Fig. 1a). No diffraction peak for metallic Ag(0) observed in Fig. 1b can be attributed to the low amount of Ag on P25, and the peak corresponding to metallic Ag(0) (1 1 1) plane at 38.1° is covered by peaks of TiO<sub>2</sub> (0 0 4) plane at 37.8° and (1 1 2) plane at 38.6° [28]. In Fig. 1c, XRD analysis of 12.5% Ag<sub>2</sub>O/P25 exhibits an apparent peak corresponding to hexagonal Ag<sub>2</sub>O (1 0 0) plane at 33.7° (JCPDS No. 72-2108). An additional peak for cubic Ag<sub>2</sub>O (1 1 1) plane is also detected at 32.6° (JCPDS No. 76-1393), suggesting that Ag<sub>2</sub>O/P25 has been successfully prepared through a pH-mediated precipitation reaction of AgNO<sub>3</sub> and NaOH at room temperature in the presence of P25.

To further identify the valence states of Ag on P25, XPS analysis was carried out (Fig. 2). The binding energy of Ag 3d<sub>5/2</sub> at oxidation states of Ag(0) and Ag(I) is always in the ranges of 368.0–368.3 eV and 367.6–367.8 eV, respectively [28,29]. Fig. 2a further demonstrates that silver mainly exists as Ag(I) in 5% Ag<sub>2</sub>O/P25, whereas F-Ag/P25 mainly contains Ag(0) (Fig. 2b).

Distribution and morphology of Ag or Ag<sub>2</sub>O particles around P25 are confirmed by TEM analysis. Fig. 3a shows that Ag(0) nanoparticles are evenly dispersed on the surface of P25, with an average diameter of ca. 3.3 nm. HRTEM image of F-Ag/P25 further reveals

that the interplanar spacing of 0.238 nm is corresponded to the (1 1 1) plane of Ag, while 0.352 nm is attributed to the (1 0 1) plane of anatase (Fig. 3b). Fig. 3c shows that Ag<sub>2</sub>O particles with an average diameter of ca., 4.4 nm are evenly dispersed on the surface of P25. Although larger particle size of 5–20 nm Ag<sub>2</sub>O was always found on the surface of TiO<sub>2</sub> [30,31], our results suggest that smaller Ag<sub>2</sub>O particles on P25 can be obtained through the pH-mediated precipitation method. Moreover, Fig. 3d reveals a close interaction between the Ag<sub>2</sub>O and P25 in the as-prepared composite, which implies the formation of Ag<sub>2</sub>O/P25 heterojunctions.

#### 3.2. Photocatalytic reduction of nitrate by Ag<sub>2</sub>O/P25

When nitrate and formic acid were mixed in dark or irradiated conditions (UV light), no nitrate reduction occurred in the absence of photocatalyst, suggesting that formic acid was not a direct reductant under these experimental conditions. The performance of Ag<sub>2</sub>O/P25 in the reduction of nitrate is summarized in Table 1 and Fig. 4. Appropriate Ag<sub>2</sub>O coating on P25 can apparently accelerate the reduction rate of nitrate. Conversion of nitrate was dependent on the amount of Ag<sub>2</sub>O on P25, and increased with the increase of Ag<sub>2</sub>O from 1% to 12.5% (Table 1). The conversion of nitrate reached 97.2% and 97.5% with a N<sub>2</sub> selectivity of 83.1% and 82.9% in the systems of 5% Ag<sub>2</sub>O/P25 and 12.5% Ag<sub>2</sub>O/P25 after 4 h reaction, respectively. Meanwhile, nitrate reduction can be described with a pseudo first-order model (Table S1), and it proceeded 6.3-fold and 6.5-fold faster in the presence of 5% Ag<sub>2</sub>O/P25 and 12.5% Ag<sub>2</sub>O/P25 relative to P25 (Table 1). As to 20% Ag<sub>2</sub>O/P25, the conversion of nitrate was only 51.9%, which could be attributed to the decrease of the available irradiation sites on P25 covered by more Ag<sub>2</sub>O nanoparticles [30]. The proper amount of Ag<sub>2</sub>O nanoparticles can efficiently prolong the separation time of photo-generated electrons and holes and improves the photocatalytic reduction of nitrate.

Nitrate reduction and the distribution of products are also dependent on the amount of Ag<sub>2</sub>O on P25. During illumination, the concentration of nitrite increased first, and then decreased in the systems of 1%, 5% and 12.5% Ag<sub>2</sub>O/P25 (Fig. 4a–c), however, it consistently increased in 20% Ag<sub>2</sub>O/P25 (Fig. 4d). Final concentrations of nitrite increased from 0.3 to 44.6 mg L<sup>−1</sup> with the increased amount of Ag<sub>2</sub>O from 1% to 20% (Fig. 4). Final concentration of ammonium reached 11.1 mg L<sup>−1</sup> in 1% Ag<sub>2</sub>O/P25, while it was only 0.7 mg L<sup>−1</sup> in 20% Ag<sub>2</sub>O/P25 (Fig. 4a and d). Previous studies have demonstrated that photocatalytic reduction of nitrate catalyzed by metal-loaded TiO<sub>2</sub> is a step-wise process, and nitrate is reduced to nitrite first, followed by a slow reduction of nitrite to ammonium

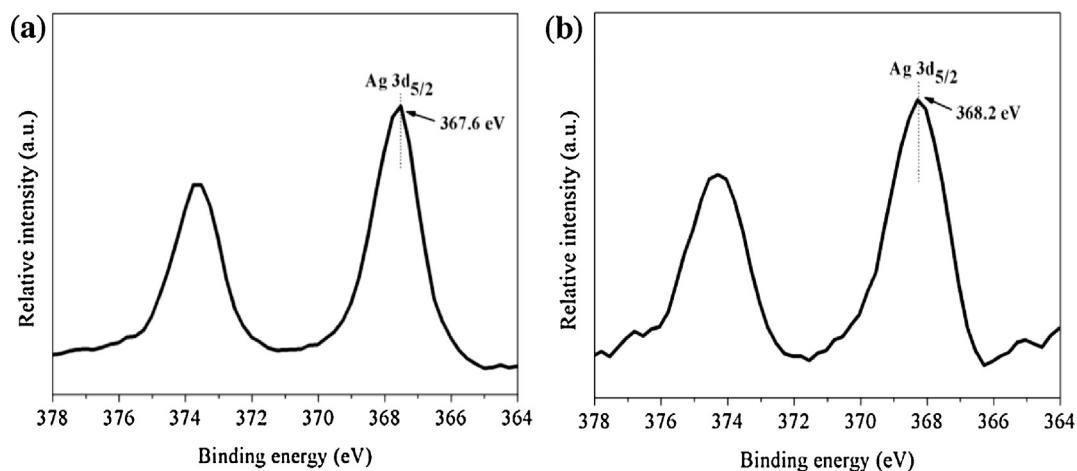
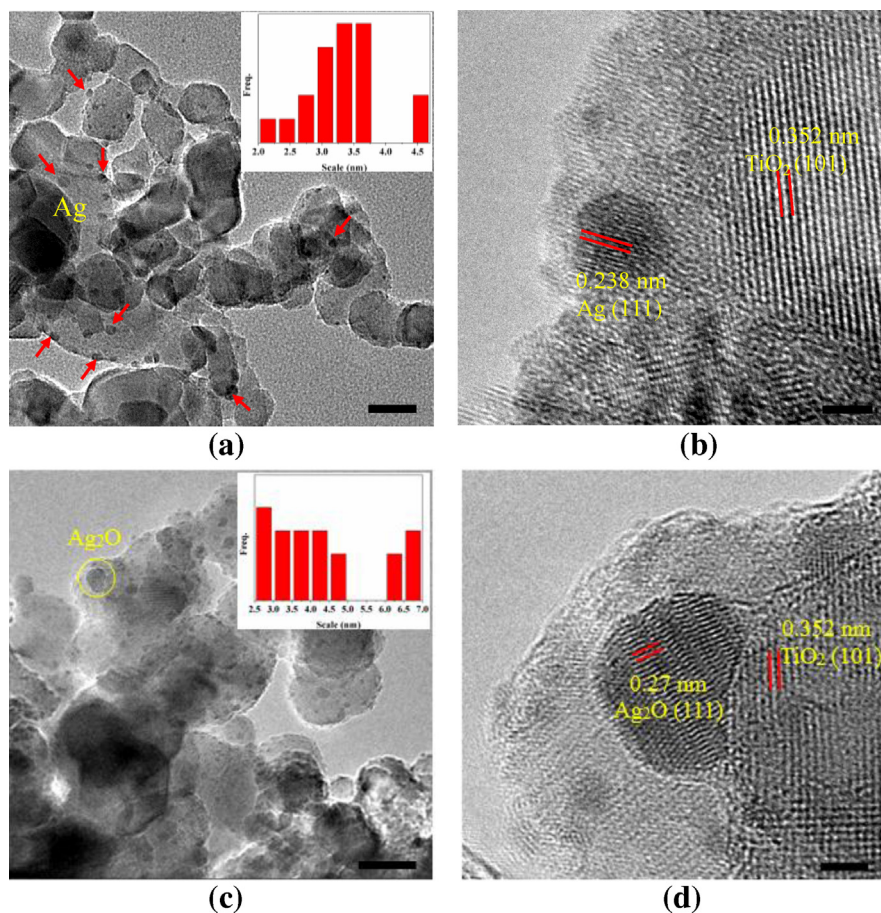


Fig. 2. Ag XPS spectra of (a) 5% Ag<sub>2</sub>O/P25 and (b) F-Ag/P25.



**Fig. 3.** TEM images of (a and b) F-Ag/P25 and (c and d) 5% Ag<sub>2</sub>O/P25. Scales are both 20 nm in (a) and (c), 5 nm in (b) and 2 nm in (d). Inserts in (a) and (c) are size distribution of Ag and Ag<sub>2</sub>O around P25 as calculated with the software of Nano Measurer, respectively.

[18,32–34]. In the system of Ag<sub>2</sub>O/P25, nitrate was first reduced to N<sub>2</sub> and nitrite, and then the formed nitrite was slowly converted to N<sub>2</sub> and ammonium. The continuous increase of nitrite in 20% Ag<sub>2</sub>O/P25 indicates that the second step of nitrite reduction to N<sub>2</sub> and ammonium was inhibited at high Ag<sub>2</sub>O loading. This can be ascribed to the decrease of the available irradiation sites on P25 covered by more Ag<sub>2</sub>O nanoparticles [30].

The reusability is an important factor to evaluate the performance of catalysts in practical application. Photocatalytic stability of Ag<sub>2</sub>O/P25 in the reduction of nitrate was investigated in the eight cycles of experiment using 5% Ag<sub>2</sub>O/P25 as the catalyst. The recycled Ag<sub>2</sub>O/P25 was centrifuged and washed repeatedly with

deionized water three times before reused in the next cycle. No obvious decrease of nitrate conversion indicates the good stability and reusability of 5% Ag<sub>2</sub>O/P25 in the reduction process (Fig. 5a). The relative contents of Ag(I) and Ag(0) in 5% Ag<sub>2</sub>O/P25 catalyst before UV irradiation were 99.3% and 0.7%, respectively, as determined by XPS analysis (Fig. S1). However, after UV irradiation, the contents of Ag(I) and Ag(0) in 5% Ag<sub>2</sub>O/P25 catalyst were 87.8% and 12.2%, respectively (Fig. S2). This demonstrates that a small fraction of Ag<sub>2</sub>O was photoreduced to Ag(0) under UV irradiation. The plasmon absorption band at 460 nm in UV–vis analysis further confirms the formation of Ag(0) nanoparticles after UV irradiation (Fig. S3) [22]. The presence of Ag(0) resulted from the reduction of Ag<sub>2</sub>O by

**Table 1**  
Conversion of nitrate, rate constant *k*, yield of nitrite and ammonium, and selectivity to N<sub>2</sub> on different catalysts.

| Catalysts                   | Substrates                           | Conversion of NO <sub>3</sub> <sup>−</sup> (%) | <i>k</i> (h <sup>−1</sup> ) | Yield of NO <sub>2</sub> <sup>−</sup> (mgN L <sup>−1</sup> ) | Yield of NH <sub>4</sub> <sup>+</sup> (mgN L <sup>−1</sup> ) | <sup>a</sup> Selectivity to N <sub>2</sub> (%) |
|-----------------------------|--------------------------------------|--|-----------------------------|--|--|--|
| P25                         | 100NO <sub>3</sub>                   | 26.8   | 0.15                        | 2.8  | 4.6  | 72.4   |
| 1% Ag <sub>2</sub> O/P25    | 100NO <sub>3</sub>                   | 77.4   | 0.96                        | 0.3  | 11.1   | 85.3   |
|                             | 100NO <sub>3</sub>                   | 97.2   | 0.95                        | 2.4  | 14.0   | 83.1   |
| 5% Ag <sub>2</sub> O/P25    | 90NO <sub>3</sub> –10NH <sub>3</sub> | 65.4   | 0.30                        | 4.7  | 18.6 (28.6) <sup>b</sup>                                     | 60.4   |
|                             | 70NO <sub>3</sub> –30NH <sub>3</sub> | 45.1   | 0.32                        | 1.4  | 4.7 (34.7) <sup>b</sup>                                      | 80.7   |
|                             | 50NO <sub>3</sub> –50NH <sub>3</sub> | 83.4   | 0.45                        | 0.8  | 25.5 (75.5) <sup>b</sup>                                     | 36.9   |
| 12.5% Ag <sub>2</sub> O/P25 | 100NO <sub>3</sub>                   | 97.5   | 0.98                        | 11.1   | 5.6  | 82.9   |
| 20% Ag <sub>2</sub> O/P25   | 100NO <sub>3</sub>                   | 51.9   | 0.15                        | 44.6   | 0.7  | 12.7   |
| F-Ag/P25 <sup>c</sup>       | 100NO <sub>3</sub>                   | 99.6   | 1.57                        | 2.3  | 9.3  | 88.4   |
| M-Ag/P25 <sup>d</sup>       | 100NO <sub>3</sub>                   | 69.7   | 0.33                        | 0.7  | 16.2   | 75.8   |

Reaction conditions: 20 mL nitrogen species solution (100 mg N L<sup>−1</sup>), 20 mg catalyst, 0.04 M formic acid and 4 h irradiation time.

<sup>a</sup> Selectivity to N<sub>2</sub> was calculated by [(converted nitrate) – nitrite – ammonium]/(converted nitrate).

<sup>b</sup> Total concentration of ammonium was shown in brackets.

<sup>c</sup> Fresh Ag/P25.

<sup>d</sup> Fresh Ag/P25 preserved for 1 month at room temperature.

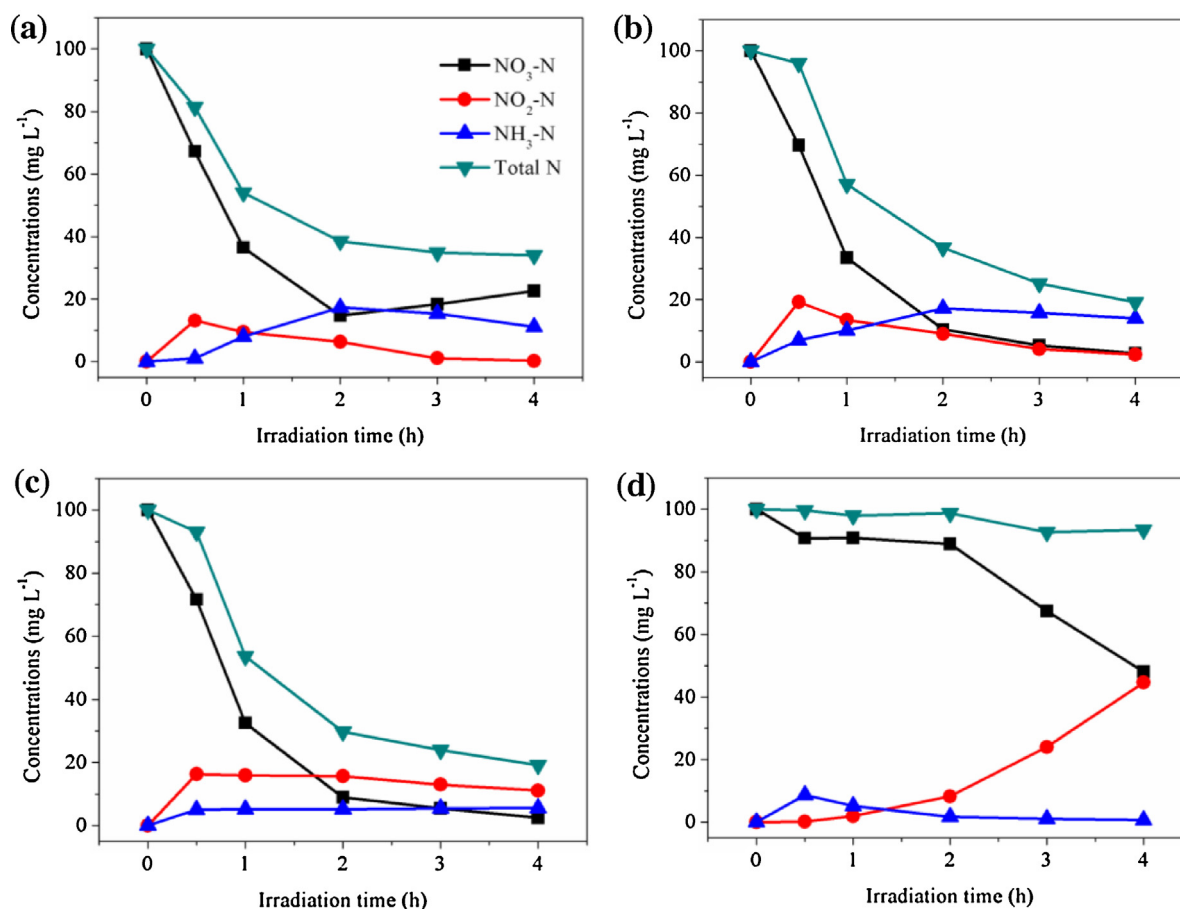


**Fig. 4.** Concentrations of  $\text{NO}_3^-$ ,  $\text{NO}_2^-$  and  $\text{NH}_4^+$  plotted as a function of irradiation time over (a) 1%  $\text{Ag}_2\text{O}/\text{P25}$ , (b) 5%  $\text{Ag}_2\text{O}/\text{P25}$ , (c) 12.5%  $\text{Ag}_2\text{O}/\text{P25}$  and (d) 20%  $\text{Ag}_2\text{O}/\text{P25}$ . Total N is the sum of  $\text{NO}_3^-$ ,  $\text{NO}_2^-$  and  $\text{NH}_4^+$ .

photo-generated electrons can effectively protect  $\text{Ag}_2\text{O}$  from complete conversion to  $\text{Ag}(0)$  under UV irradiation. Previous studies also suggested that  $\text{Ag}_2\text{O}$  nanoparticles exhibited self-stability once the  $\text{Ag}-\text{Ag}_2\text{O}$  structure was formed during the photo-degradation process [22,35].

Photocatalytic nitrate reduction by  $\text{Ag}/\text{P25}$  was also conducted to make a comparison with  $\text{Ag}_2\text{O}/\text{P25}$ . The conversion of nitrate was 99.6% with a  $\text{N}_2$  selectivity of 88.4% in F- $\text{Ag}/\text{P25}$  after 4 h reaction (Table 1). F- $\text{Ag}/\text{P25}$  not only showed a high activity in nitrate reduction ( $12.45 \text{ mg}_{\text{NO}_3^-} \text{ h}^{-1} \text{ g}_{\text{cat}}^{-1}$ , 3.72 times of P25), but also exhibited a high  $\text{N}_2$  selectivity (1.22 times of P25). However, conversion of nitrate was only 69.7% with a  $\text{N}_2$  selectivity of 75.8% in the presence of M- $\text{Ag}/\text{P25}$  after 4 h reaction. To the best of our knowledge, no work has been done to investigate the repeated use of  $\text{Ag}/\text{TiO}_2$  in the photocatalytic reduction of nitrate, although many studies have mentioned its high efficiency in nitrate reduction [17–19]. Four cycles of photo-reduction of nitrate were conducted using F- $\text{Ag}/\text{P25}$  to evaluate the photocatalytic stability of  $\text{Ag}/\text{P25}$  catalyst. Fig. 5b shows that there was a remarkable decrease in the reduction efficiency during the recycling experiment. The conversion of nitrate decreased to 11.7% in the fourth cycle (Fig. 5b), suggesting that  $\text{Ag}/\text{P25}$  was not appropriate for the practical application due to its weak reusability. The XPS analysis shows the presence of  $\text{Ag}(I)$  on F- $\text{Ag}/\text{P25}$  after photocatalytic reduction of nitrate (Fig. S4). The decreased catalytic capacity of  $\text{Ag}/\text{P25}$  during recycling experiment was therefore due to partial oxidation of  $\text{Ag}(0)$  to  $\text{Ag}(I)$  by dissolved oxygen [36], which resulted in the formation of  $\text{Ag}_2\text{O}$  on the surface of  $\text{Ag}(0)$ .

### 3.3. Influence of ammonium on photocatalytic reduction of nitrate or nitrite by $\text{Ag}_2\text{O}/\text{P25}$

Previous studies always focused the photocatalytic reduction of a single nitrogen species such as nitrate or nitrite, however, two or more inorganic nitrogen species always coexist in wastewater [37,38]. We hereby investigated the presence of ammonium on the reduction of nitrate by 5%  $\text{Ag}_2\text{O}/\text{P25}$ . The presence of ammonium effectively inhibited the reduction of nitrate (Figs. 4b and 6a–c). With the increase of ammonium from 0 to  $10 \text{ mg L}^{-1}$ , the conversion of nitrate decreased from 97.2% to 65.4% and the pseudo first-order rate constant also decreased from  $0.95$  to  $0.3 \text{ h}^{-1}$  (Table 1). More interestingly, there was almost no nitrite detected in these reactions (Fig. 6a–c), which indicates that the pre-existed ammonium inhibited the yield of nitrite, and nitrate could be directly converted to ammonium and  $\text{N}_2$  in the presence of high concentrations of ammonium (Table 1).

The photocatalytic reduction of nitrite by 5%  $\text{Ag}_2\text{O}/\text{P25}$  was also conducted in the absence and presence of ammonium (Fig. 6d–f). Compared with the results in the absence of ammonium, final conversion of nitrite did not show significant differences after 4 h reaction (Table 2). However, ammonium could accelerate the rate of nitrite reduction, and almost 100% conversion of nitrite could be accompanied in the presence of ammonium in the first 0.5 h (Fig. 6d and e). Compared with pure nitrite system, the photocatalytic reduction of nitrite preceded 3.2-fold and 2.9-fold faster in the presence of 25 and  $50 \text{ mg L}^{-1}$  ammonium, respectively (Table 2).

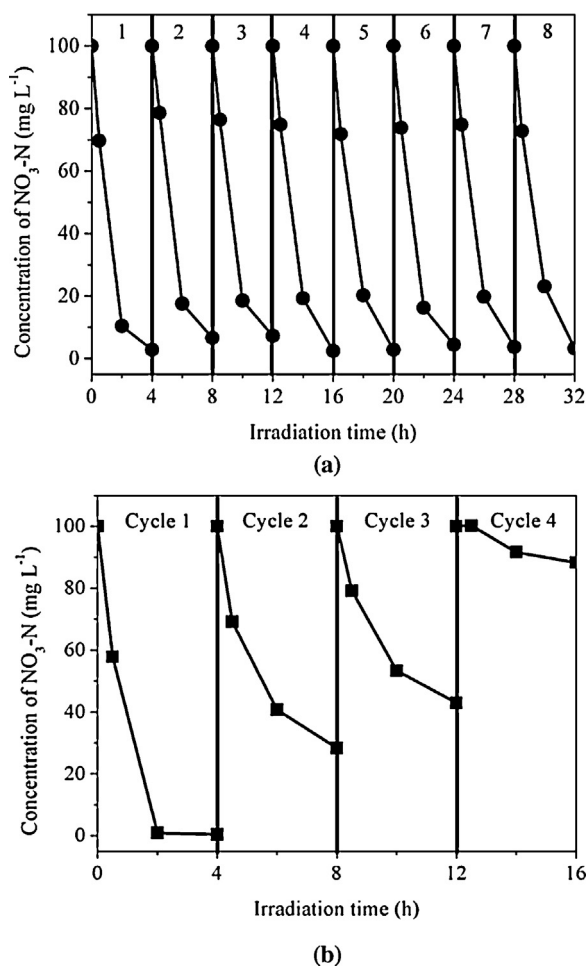


Fig. 5. Recycled uses of (a) 5% Ag<sub>2</sub>O/P25 and (b) F-Ag/P25 in the photocatalytic reduction of nitrate.

Unexpectedly, a small fraction of nitrite was also oxidized to nitrate in the first 0.5 h. The hydroxyl free radicals ( $\bullet\text{OH}$ ) produced by irradiation in the presence of oxygen and titanium dioxide play an important role to oxidize nitrite to nitrate [39]. To further verify the  $\bullet\text{OH}$ -mediated oxidation, the influence of scavenger methanol was added in the system. The results indicate that excess methanol (1 M) inhibited the oxidation of nitrite to nitrate (Fig. S5). At the same time, almost no oxidation of ammonium in Fig. S6 further indicated that the formation of nitrate should result from the oxidation of nitrite but not ammonium. With the increased addition of ammonium, final concentrations of nitrate decreased from 11.9 to 4.0 mg L<sup>-1</sup>, implying that the presence of ammonium could inhibit the formation of nitrate during nitrite reduction (Table 2). Meanwhile, the presence of ammonium decreased the N<sub>2</sub> selectivity, and the values were 68.6% and 62.7% when the concentrations of ammonium were 25 and 50 mg L<sup>-1</sup>, respectively.

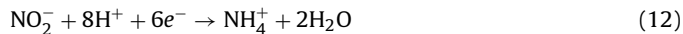
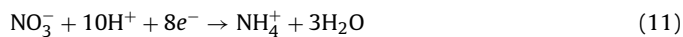
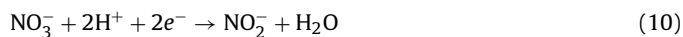
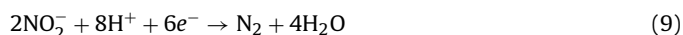
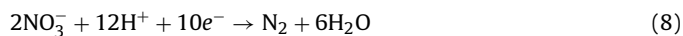
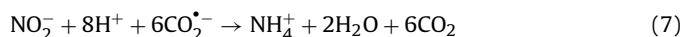
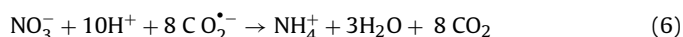
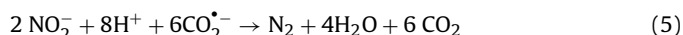
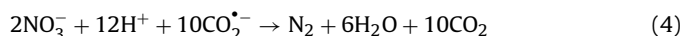
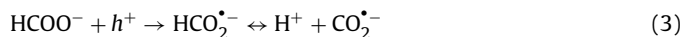
#### 3.4. Mechanisms involved in the photocatalytic reduction of nitrate

Ag<sub>2</sub>O/P25 shows good performances in the reduction of nitrate (Figs. 4 and 6), and the mechanism involved in this process is shown in Scheme 1a. When Ag<sub>2</sub>O/P25 is illuminated by UV light, both Ag<sub>2</sub>O and P25 can be excited to form electron-hole pairs according to Eqs. (1) and (2).



As mentioned in previous study [31], due to band bending and under the influence of the electrostatic field  $\xi$  in the junction of Ag<sub>2</sub>O and P25, photo-generated electrons could move from Ag<sub>2</sub>O to conduction band of P25 and photo-generated holes could move from P25 to valence band of Ag<sub>2</sub>O, which promotes the interfacial electron transfer rate and suppresses the charge recombination on the semiconductor.

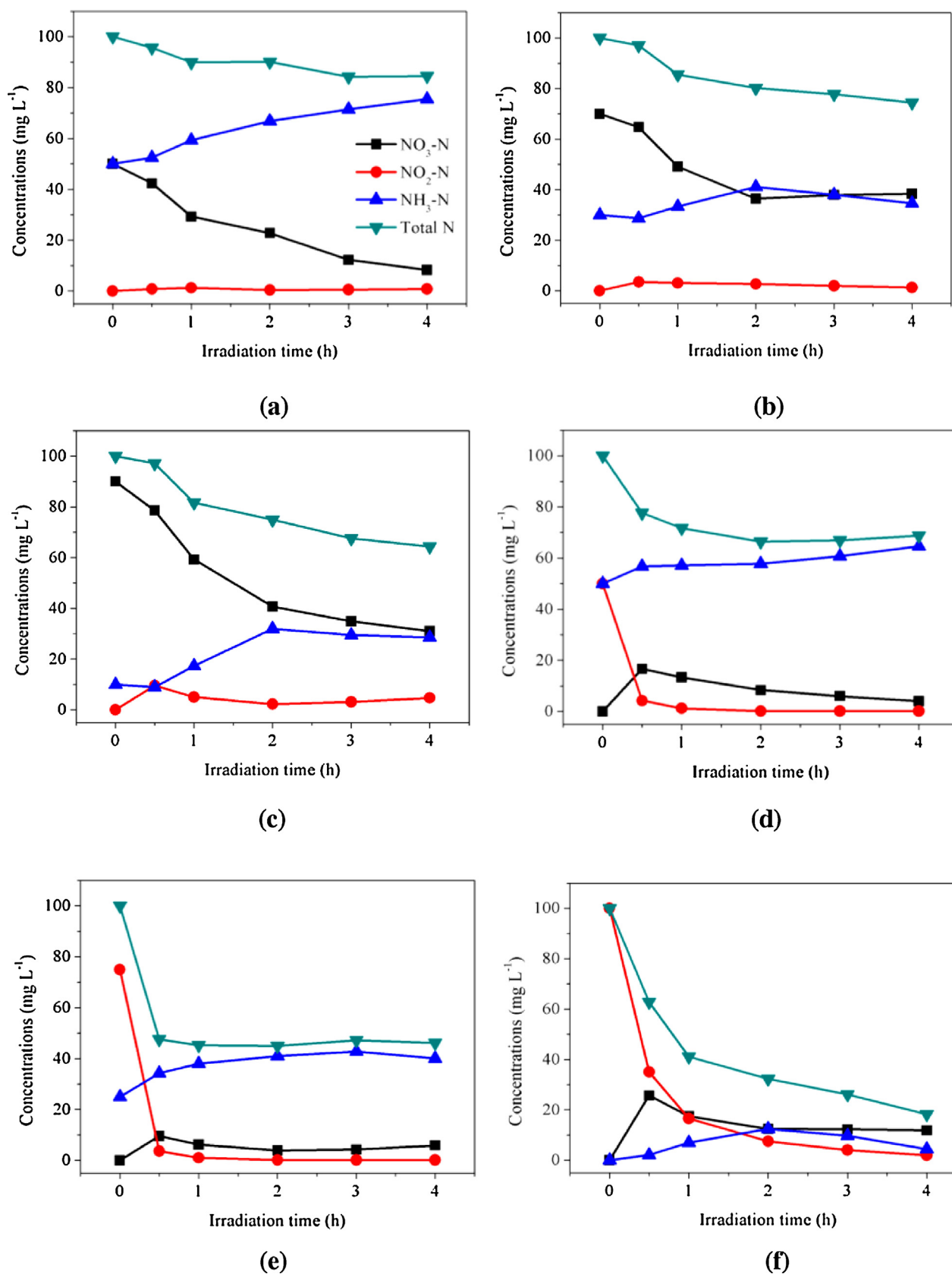
Subsequently, photo-generated electrons and holes can be consumed by nitrate and formic acid, respectively. Electron paramagnetic resonance (EPR) analysis demonstrates that the photo-generated holes are consumed by formic anions to form CO<sub>2</sub> $\bullet^-$  [Eq. (3)] [40]. The CO<sub>2</sub> $\bullet^-$  species shows a strong reductive ability ( $E^\ominus(\text{CO}_2/\text{CO}_2\bullet^-) = -1.8\text{ V}$ ) [41] in the reduction of nitrate and nitrite to N<sub>2</sub> ( $E^\ominus(\text{NO}_3^-/\text{N}_2) = 1.25\text{ V}$ ;  $E^\ominus(\text{NO}_2^-/\text{N}_2) = 1.45\text{ V}$ ) [Eqs. (4) and (5)] or to ammonium ( $E^\ominus(\text{NO}_3^-/\text{NH}_4^+) = 1.203\text{ V}$ ;  $E^\ominus(\text{NO}_2^-/\text{NH}_4^+) = 0.897\text{ V}$ ) [Eqs. (6) and (7)] [17,42]. The photo-generated electrons also have a weak ability to reduce nitrate and nitrite [Eqs. (8)–(12)]. Doudrick et al. [18] have demonstrated that electrons could be used for photocatalytic reduction of nitrate. Because no treatment was taken to deal with the dissolved oxygen during the reaction, the reduction of nitrate and nitrite might compete by the oxidation of nitrite by oxygen ( $E^\ominus(\text{O}_2/\text{H}_2\text{O}) = 1.23\text{ V}$ ;  $E^\ominus(\text{NO}_3^-/\text{NO}_2^-) = 0.94\text{ V}$ ). Considering nitrate is a more effective electron scavenger than oxygen [43], oxidation of nitrite to nitrate by oxygen is unlikely to be predominant, and nitrate reduction could be apparently observed in the presence of oxygen in this study.



It is expected that if the photo-generated holes in Ag<sub>2</sub>O/P25 can transfer to formic acid before oxidizing the O(-II) in Ag<sub>2</sub>O and the photo-generated electrons are captured by nitrate before reducing Ag(I), it is possible to keep the stability of Ag–O–Ag in Ag<sub>2</sub>O under light irradiation. The outstanding reusability of this catalyst can be due to the good stability of Ag<sub>2</sub>O during the recycled processes [22], which suggests that Ag<sub>2</sub>O/P25 can be used in practical application.

Meanwhile, the mechanism involved in the photocatalytic reduction of nitrate by F-Ag/P25 is described in Scheme 1b. When P25 is irradiated under UV light with photon energy equal or higher to the band gap of P25 (3.2 eV), it will be excited to form electron-hole pairs [Eq. (1)], and the loaded Ag on TiO<sub>2</sub> works as electron traps and aids the separation of electron-hole pairs [17–19]. The reduction of nitrate by F-Ag/P25 can occur: (i) via reaction with CO<sub>2</sub> $\bullet^-$  radical produced from the reaction between photo-generated holes and formic acid, and (ii) by direct interaction of the reactants with electrons reaching the surface of semiconductor.

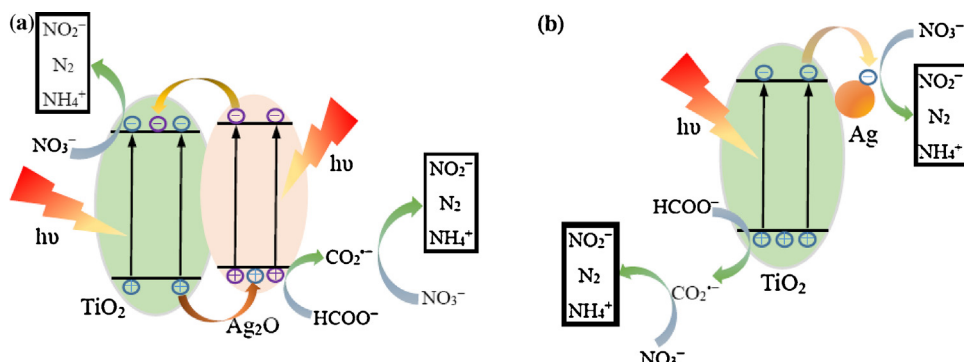
In the photocatalytic reduction of nitrate by 5% Ag<sub>2</sub>O/P25, the deposited Ag<sub>2</sub>O species are partially photoreduced and the formed Ag–Ag<sub>2</sub>O structure [the Ag(0) present on the surface of Ag<sub>2</sub>O] over P25 contributes to the better activity and stability of this catalyst.



**Fig. 6.** Concentrations of  $\text{NO}_3^-$ ,  $\text{NO}_2^-$  and  $\text{NH}_4^+$  plotted as a function of irradiation time over 5%  $\text{Ag}_2\text{O}/\text{P25}$ . (a)  $[\text{NO}_3^-]_0 = [\text{NH}_4^+]_0 = 50 \text{ mg L}^{-1}$ , (b)  $[\text{NO}_3^-]_0 = 70 \text{ mg L}^{-1}$ ,  $[\text{NH}_4^+]_0 = 30 \text{ mg L}^{-1}$ , (c)  $[\text{NO}_3^-]_0 = 90 \text{ mg L}^{-1}$ ,  $[\text{NH}_4^+]_0 = 10 \text{ mg L}^{-1}$ , (d)  $[\text{NO}_2^-]_0 = [\text{NH}_4^+]_0 = 50 \text{ mg L}^{-1}$ , (e)  $[\text{NO}_2^-]_0 = 75 \text{ mg L}^{-1}$ ,  $[\text{NH}_4^+]_0 = 25 \text{ mg L}^{-1}$  and (f)  $[\text{NO}_2^-]_0 = 100 \text{ mg L}^{-1}$ . Total N is the sum of  $\text{NO}_3^-$ ,  $\text{NO}_2^-$  and  $\text{NH}_4^+$ .

**Table 2**Conversion of nitrite, rate constant  $k$ , yield of nitrate and ammonium, and selectivity to  $N_2$  on 5%  $Ag_2O/P25$ .

| Substrates           | Conversion of $NO_2^-$ (%) | $k$ ( $h^{-1}$ ) | Yield of $NO_3^-$ ( $mgNL^{-1}$ ) | Yield of $NH_4^+$ ( $mgNL^{-1}$ ) | <sup>a</sup> Selectivity to $N_2$ (%) |
|----------------------|----------------------------|------------------|-----------------------------------|-----------------------------------|---------------------------------------|
| 50 $NO_2$ –50 $NH_3$ | 99.6                       | 3.10             | 4.0                               | 14.6 (64.6) <sup>b</sup>          | 62.7                                  |
| 75 $NO_2$ –25 $NH_3$ | 99.8                       | 3.45             | 5.9                               | 15.1 (40.1) <sup>b</sup>          | 68.6                                  |
| 100 $NO_2$           | 98.0                       | 1.08             | 11.9                              | 4.4                               | 83.4                                  |

Reaction conditions: 20 mL nitrogen species solution ( $100\text{ mg } N L^{-1}$ ), 20 mg catalyst, 0.04 M formic acid and 4 h irradiation time.<sup>a</sup> Selectivity to  $N_2$  was calculated by [(converted nitrite) – nitrate – ammonium]/(converted nitrite).<sup>b</sup> Total concentration of ammonium was shown in brackets.**Scheme 1.** The proposed photocatalytic mechanisms of (a) 5%  $Ag_2O/P25$  and (b) F-Ag/P25 in nitrate reduction.

Considering  $Ag(0)$  nanoparticles can be easily oxidized to  $Ag_2O$ , the structure of  $Ag_2O-Ag$  [the  $Ag_2O$  present on the surface of  $Ag(0)$ ] on P25 was formed in M-Ag/P25 as confirmed in our study. The relative content of  $Ag(I)$  in 5%  $Ag_2O/P25$  after UV irradiation (87.8%) and M-Ag/P25 (90.0%) is comparable (Figs. S2 and S7), but the activity is different (the conversion of nitrate was only 69.7% with a  $N_2$  selectivity of 75.8% for the latter). Therefore, for the photocatalytic reduction of nitrate, the differences on the activity and selectivity in the systems of Ag/P25 and  $Ag_2O/P25$  can be attributed to the different structures of  $Ag_2O-Ag$  and  $Ag-Ag_2O$  on P25.

As to semiconductor nanocomposites, photoluminescence (PL) spectra of the catalysts can provide information on the separation and recombination of photo-induced charge carriers [30]. Fig. 7 shows the PL spectra of neat P25, M-Ag/P25 and 5%  $Ag_2O/P25$  in the range of 350–550 nm with the excitation wavelength at 325 nm. The neat P25 has a strong emission peak at about 410 nm (Fig. 7a). With the deposition of  $Ag(0)$  and exposed to air for one month, the PL intensity of M-Ag/P25 decreased (Fig. 7b). The emission peak

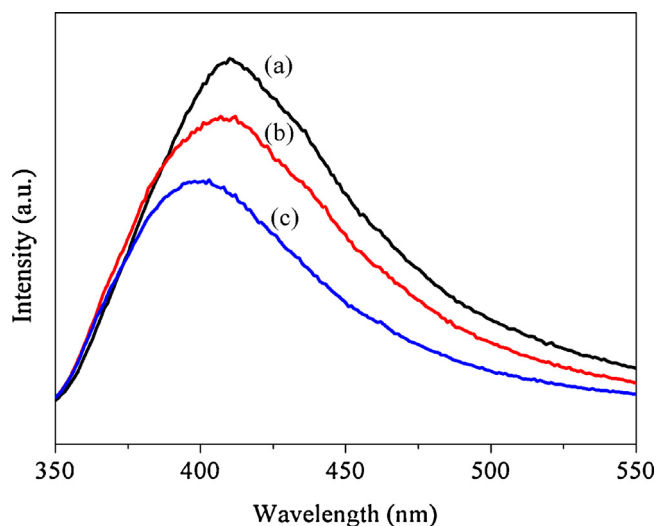
position of 5%  $Ag_2O/P25$  decreased to 402 nm and the intensity further decreased due to the deposition of  $Ag_2O$  (Fig. 7c). Previous study also demonstrated that the presence of  $Ag_2O$  resulted in the decrease of emission peak position in comparison with pure  $TiO_2$  [44]. Considering PL intensities are opposite to the photocatalytic activities, Fig. 7 further demonstrates that photocatalytic reduction efficiency for nitrate is 5%  $Ag_2O/P25 > M-Ag/P25 > P25$ , which are consistent to the results shown in Table 1.

In order to investigate the dissolved oxygen on the reduction of nitrate in this study, photocatalytic nitrate reduction by 5%  $Ag_2O/P25$  was conducted in the absence of dissolved oxygen via continuous nitrogen bubbling. After 4 h reaction, the conversion of nitrate was 96.5% with a  $N_2$  selectivity of 71.1% (Fig. S8). We therefore, conclude that the dissolved oxygen does not inhibit nitrate reduction.

Photocatalytic reduction of nitrate by F-Ag/P25 and 5%  $Ag_2O/P25$  was also conducted under visible light irradiation [the visible light was provided by a 500 W Xe lamp with a UV cutoff filter ( $\lambda > 420\text{ nm}$ )], and the results suggest that nitrate reduction under visible light irradiation can be neglected (Fig. S9).

#### 4. Conclusions

$Ag_2O/P25$ , an easy prepared catalyst was synthesized in this study, and was applied into the photocatalytic reduction of nitrate in the presence of formic acid. XRD, XPS and TEM analysis show that  $Ag_2O$  nanoparticles are well distributed on the surface of P25. Under UV irradiation, 5%  $Ag_2O/P25$  shows a fast rate ( $0.95\text{ h}^{-1}$ , 6.3 times of P25), a high conversion (97.2%, 3.63 times of P25) and a high  $N_2$  selectivity (83.1%, 1.15 times of P25) for nitrate reduction. The improved separation of electron–hole pairs on  $Ag_2O/P25$  results in the high conversion of nitrate. The distribution of final products is strongly dependent on the amount of  $Ag_2O$  loaded on P25. In addition, the presence of ammonium inhibits the conversion of nitrate apparently, but accelerates the reduction rate of nitrite. The better stability and reusability of  $Ag_2O/P25$  (the formed  $Ag-Ag_2O$  structure) than those of Ag/P25 (the formed  $Ag_2O-Ag$  structure) after repeated cycles in the reduction of nitrate suggest that  $Ag_2O/P25$  is more appropriate for the practical application. The present study

**Fig. 7.** Photoluminescence (PL) spectra of (a) P25, (b) M-Ag/P25 and (c) 5%  $Ag_2O/P25$ .

provides a new sight into the use of Ag<sub>2</sub>O/P25 catalyst in the reduction of nitrate.

## Acknowledgments

We greatly acknowledge the financial support from the National Natural Science Foundation of China (No. 41003040, No. 41373114 and No. 41201487), and the Open Funding Project of the Key Laboratory of Systems Bioengineering, Ministry of Education. We are also grateful for the Program of Introducing Talents of Discipline to Universities (No. B06006).

## Appendix A. Supplementary data

Supplementary data associated with this article can be found, in the online version, at <http://dx.doi.org/10.1016/j.apcatb.2015.03.038>.

## References

- [1] A. Bhatnagar, M. Sillanpää, *Chem. Eng. J.* 168 (2011) 493–504.
- [2] M. Shand, J.A. Anderson, *Catal. Sci. Technol.* 3 (2013) 879–899.
- [3] U.S. Environmental Protection Agency, Drinking Water Standards and Health Advisories, US Environmental Protection Agency, Office of Water, 2000, 822-B-00-001.
- [4] O. Primo, M.J. Rivero, A.M. Urriaga, I. Ortiz, *J. Hazard. Mater.* 164 (2009) 389–393.
- [5] C.T. Matos, S. Velizarov, J.G. Crespo, M.A.M. Reis, *Water Res.* 40 (2006) 231–240.
- [6] L.A. Richards, M. Vuachère, A.I. Schäfer, *Desalination* 261 (2010) 331–337.
- [7] N. Barrabés, J. Sá, *Appl. Catal. B: Environ.* 104 (2011) 1–5.
- [8] K.D. Vorlop, T. Tacke, *Chem. Ing. Tech.* 61 (1989) 836–837.
- [9] A. Pintar, J. Batista, *Catal. Today* 53 (1999) 35–50.
- [10] A.E. Palomares, J.G. Prato, F. Rey, A. Corma, *J. Catal.* 221 (2004) 62–66.
- [11] J. Hirayama, Y. Kamiya, *ACS Catal.* 4 (2014) 2207–2215.
- [12] W.L. Gao, R.C. Jin, J.X. Chen, X.X. Guan, H.S. Zeng, F.X. Zhang, N.J. Guan, *Catal. Today* 90 (2004) 331–336.
- [13] K.T. Ranjit, B. Viswanathan, *J. Photochem. Photobiol. A: Chem.* 108 (1997) 73–78.
- [14] H. Kominami, T. Nakaseko, Y. Shimada, A. Furusho, H. Inoue, S. Murakami, Y. Kera, B. Ohtani, *Chem. Commun.* 23 (2005) 2933–2935.
- [15] J.A. Anderson, *Catal. Today* 175 (2011) 316–321.
- [16] J.A. Anderson, *Catal. Today* 181 (2012) 171–176.
- [17] F.X. Zhang, R.C. Jin, J.X. Chen, C.Z. Shao, W.L. Gao, L.D. Li, N.J. Guan, *J. Catal.* 232 (2005) 424–431.
- [18] K. Doudrick, T. Yang, K. Hristovski, P. Westerhoff, *Appl. Catal. B: Environ.* 136 (2013) 40–47.
- [19] J. Sá, C.A. Agüera, S. Gross, J.A. Anderson, *Appl. Catal. B: Environ.* 85 (2009) 192–200.
- [20] A. Takai, P.V. Kamat, *ACS Nano* 5 (2011) 7369–7376.
- [21] L.M. Lyu, M.H. Huang, *J. Phys. Chem. C* 115 (2011) 17768–17773.
- [22] X.F. Wang, S.F. Li, H.G. Yu, J.G. Yu, S.W. Liu, *Chem. Eur. J.* 17 (2011) 7777–7780.
- [23] G. Wang, X.C. Ma, B.B. Huang, H.F. Cheng, Z.Y. Wang, J. Zhan, X.Y. Qin, X.Y. Zhang, Y. Dai, *J. Mater. Chem.* 22 (2012) 21189–21194.
- [24] S. Rengaraj, X.Z. Li, *Chemosphere* 66 (2007) 930–938.
- [25] H. Kominami, A. Furusho, S.Y. Murakami, H. Inoue, Y. Kera, B. Ohtani, *Catal. Lett.* 76 (2001) 31–34.
- [26] L.L. Perissinotti, M.A. Brusa, M.A. Grela, *Langmuir* 17 (2001) 8422–8427.
- [27] D.F. Boltz, J.A. Howell, *Colorimetric Determination of Non-Metal*, Wiley, New York, 1978.
- [28] X.F. You, F. Chen, J.L. Zhang, M. Anpo, *Catal. Lett.* 102 (2005) 247–250.
- [29] E.P. Meliána, O.G. Díaz, J.M.D. Rodríguez, G. Colónb, J.A. Naviob, M. Macíasb, J.P. Peña, *Appl. Catal. B: Environ.* 127 (2012) 112–120.
- [30] W.J. Zhou, H. Liu, J.Y. Wang, D. Liu, G.J. Du, J.J. Cui, *ACS Appl. Mater. Interfaces* 2 (2010) 2385–2392.
- [31] D. Sarkar, C.K. Ghosh, S. Mukherjee, K.K. Chattopadhyay, *ACS Appl. Mater. Interfaces* 5 (2013) 331–337.
- [32] K.T. Ranjit, T.K. Varadarajan, B. Viswanathan, *J. Photochem. Photobiol. A: Chem.* 89 (1995) 67–68.
- [33] N. Wehbe, M. Jaafar, C. Guillard, J.M. Herrmann, S. Miachon, E. Puzenat, N. Guilhaume, *Appl. Catal. A: Gen.* 368 (2009) 1–8.
- [34] A. Kudo, K. Domen, K. Maruya, T. Onishi, *J. Catal.* 135 (1992) 300–303.
- [35] H.G. Yu, R. Liu, X.F. Wang, P. Wang, J.G. Yu, *Appl. Catal. B: Environ.* 111 (2012) 326–333.
- [36] K. Awazu, M. Fujimaki, C. Rockstuhl, J. Tominaga, H. Murakami, Y. Ohki, N. Yoshida, T. Watanabe, *J. Am. Chem. Soc.* 130 (2008) 1676–1680.
- [37] L.F. Liu, X.T. Li, F.L. Yang, J.C. Yu, *Photogr. Sci. Photochem.* 24 (2006) 291–300.
- [38] L.F. Liu, Y. Zhang, F.L. Yang, G.H. Chen, J.C. Yu, *Sep. Purif. Technol.* 67 (2009) 244–248.
- [39] K. Tennakone, S. Punchihewa, R.U. Tantrigoda, *Environ. Pollut.* 57 (1989) 299–305.
- [40] J.R. Harbour, M.L. Hair, *J. Phys. Chem.* 83 (1979) 652–656.
- [41] W.H. Koppenol, J.D. Rush, *J. Phys. Chem.* 91 (1987) 4429–4430.
- [42] L.F. Liu, X.Y. Dong, F.L. Yang, J.C. Yu, *Chin. J. Inorg. Chem.* 24 (2008) 211–217.
- [43] S.T. Martin, H. Herrmann, M.R. Hoffmann, *J. Chem. Soc. Faraday Trans.* 90 (1994) 3323–3330.
- [44] W.J. Zhou, H. Liu, J.Y. Wang, D. Liu, G.J. Du, S.J. Han, J.J. Lin, R.J. Wang, *Phys. Chem. Chem. Phys.* 12 (2010) 15119–15123.